Uncalibrated Visual Servoing Using More Precise Model

Qingshan Fu, Zhisheng Zhang, Jinfei Shi
School of Mechanical Engineering
Southeast University
Nanjing, China
qsfu99@163.com, oldbc@seu.edu.cn, shijf@seu.edu.cn

***Abstract*—A visual servoing method using a more precise model is presented in this paper. It uses a secant to approximate the second order term in the Hessian of the Newton model. This is different from the popular so-called quasi-Newton uncalibrated visual servoing method, which neglects the second order term directly. Its performance is superior to the so-called quasi-Newton uncalibrated visual servoing method, especially in large residual cases. To guarantee the global convergence of this method, a trust region method is used. Besides, a recursive least squares algorithm is employed to estimate the coupled image Jacobian, so it is not necessary to know the parameters of the camera and the robot. More than that, an approach to improving the control precision of the end-effector in the workspace is also proposed. In the end, a three-degree-of-freedom robot with two fixed cameras system is simulated to validate the method. The simulation results demonstrate the effectiveness of the method.**

***Keywords*—uncalibrated visual servoing, large residual, jacobian estimation, robot.**

I. INTRODUCTION

Most of visual servoing methods in previous works need to calibrate the camera and the robot. A set of calibration movements have to be made for the calibration and it is needed to recalibrate frequently. However, these movements are not necessary for our task, sometimes, even interfering with our task. Moreover, in many circumstances, it is very difficult to calibrate them exactly or unable to calibrate them at all.

Hosoda et al. [1] proposed an uncalibrated visual servoing method in which least squares algorithm with exponential data weighting was used to estimate the coupled image Jacobian. Jagersand [2] developed a static quasi-Newton uncalibrated visual servoing method. In this method, Broyden's method is used to estimate the coupled image Jacobian, and a trust region method is employed to adjust the step length so that each step is maximal while maintaining convergence. The uncalibrated visual servoing methods mentioned above are just fit for stationary targets. Piepmeier et al. [3][4] proposed a dynamic qusi-Newton uncalibrated visual servoing method. It is fit for both moving targets and stationary targets. Besides, researchers proposed many other methods. For example, Jiang et al. [5] put forward an indirect iterative learning control method for a discrete visual servo without a camera-robot model. Liu et al. [6] proposed an uncalibrated visual servoing method using a depth-independent interaction matrix. Among all of these methods, the quasi-Newton uncalibrated visual servoing method is quite popular. However, the so-called quasi-Newton uncalibrated visual servoing method, exactly, is a Gauss-Newton method. It drops the second order term directly. In zero residual, small residual or the low degree of nonlinearity cases, it is quadratic or nearly quadratic convergent; But in large residual or high degree of nonlinearity cases, the method sometimes can't converge or converges very slowly. Additionally, Gauss-Newton method needs that the Jacobian matrix is full rank, otherwise the method makes no sense. In fact, the singularity of Jacobian matrix occurs frequently. Besides, Gauss-Newton method is not globally convergent.

For the shortcomings of Gauss-Newton method, Miura et al. [7] put forward an uncalibrated visual servoing method using modified simplex optimization. It is globally convergent. However, the estimation of Jacobian is not accurate because of the large motions of the robot between the vertices of the simplex, which may lead to low precision of the robot control. Kim et al. [8] proposed an uncalibrated visual serving method for large residual problems. It uses a secant to approximate the second order term rather than dropping it directly. However, the method to compute the second order term destroys much information. This may lead to instability of the method.

A new uncalibrated visual servoing method for large residual problems is developed in this paper. It also uses a secant to approximate the second order term, but the method to compute the second order term is different from Kim's, it destroys the least information, so it is much more stable. Besides, a trust region method, which guarantees the global convergence of this method, is used. More than that, a method to improve the control precision in the workspace is proposed. This is much different from previous works, for they are mainly concerned with the control precision in the image plane. In practice, the control precision in the workspace is our real concern. In the end, a three-degree-of-freedom robot is simulated to validate the control algorithm.

II. UNCALIBRATED VISUAL SERVOING USING GAUSS-NEWTON METHOD

Let $\boldsymbol{\theta}$ be the current joint angles, $\boldsymbol{\theta}^*$ be the desired joint angles, where $\boldsymbol{\theta} \in R^n$, $\boldsymbol{\theta}^* \in R^n$, n is the number of degrees of freedom of the robot; Current feature vector and desired feature vector in the image plane are denoted by $\boldsymbol{y}$ and $\boldsymbol{y}^*$, respectively, where $\boldsymbol{y} \in R^m$, $\mathbf{y}^* \in R^m$, m is the number of features. When the end-effector changes from current pose to desired pose, the joint angles changes from $\boldsymbol{\theta}$ to $\boldsymbol{\theta}^*$ and the feature vector changes from $\boldsymbol{y}$ to $\boldsymbol{y}^*$. The error in the image plane is $\boldsymbol{f} = \mathbf{y} - \mathbf{y}^*$. Constructing a least squares objective function

$$\Phi = \frac{1}{2}\boldsymbol{f}^T\boldsymbol{f} \quad (1)$$

Then, the control problem of driving the joints from $\boldsymbol{\theta}$ to $\boldsymbol{\theta}^*$ is transformed into solving the least squares problem.

Let J be the Jacobian of $\boldsymbol{f}$. Then, the gradient of Φ is

$$\mathbf{g} = \mathbf{J}^T\boldsymbol{f} \quad (2)$$

and the Hessian of Φ is

$$\mathbf{G} = \mathbf{J}^T\mathbf{J} + \mathbf{S} \quad (3)$$

where $\mathbf{S} = \sum_{i=1}^{m} \boldsymbol{f}_i \nabla^2 \boldsymbol{f}_i$.

The Taylor series expansion about $\boldsymbol{\theta}$ is

$$\begin{aligned}\Phi &= \Phi_k + \boldsymbol{g}_k{}^T(\boldsymbol{\theta} - \boldsymbol{\theta}_k) \\ &+ \frac{1}{2}(\boldsymbol{\theta} - \boldsymbol{\theta}_k)^T \boldsymbol{G}_k(\boldsymbol{\theta} - \boldsymbol{\theta}_k) + \ldots\end{aligned} \quad (4)$$

Dropping the higher order terms we get the quadratic model

$$q_k = \Phi_k + \boldsymbol{g}_k{}^T(\boldsymbol{\theta} - \boldsymbol{\theta}_k) + \frac{1}{2}(\boldsymbol{\theta} - \boldsymbol{\theta}_k)^T \boldsymbol{G}_k(\boldsymbol{\theta} - \boldsymbol{\theta}_k) \quad (5)$$

Substituting (2) and (3) into (5), yield

$$\begin{aligned}q_k &= \frac{1}{2}\boldsymbol{f}_k^T\boldsymbol{f}_k + (\mathbf{J}_k^T\boldsymbol{f}_k)^T(\boldsymbol{\theta} - \boldsymbol{\theta}_k) \\ &+ \frac{1}{2}(\boldsymbol{\theta} - \boldsymbol{\theta}_k)^T(\mathbf{J}_k^T\mathbf{J}_k + \mathbf{S}_k)(\boldsymbol{\theta} - \boldsymbol{\theta}_k)\end{aligned} \quad (6)$$

The Newton's method to minimize q_k is

$$\boldsymbol{\theta}_{k+1} = \boldsymbol{\theta}_k - (\mathbf{J}_k^T\mathbf{J}_k + \mathbf{S}_k)^{-1}\mathbf{J}_k^T\boldsymbol{f}_k \quad (7)$$

$\mathbf{S}_k$ is very difficult to compute. So, it is often dropped. Then, the method becomes the Gauss-Newton method

$$\boldsymbol{\theta}_{k+1} = \boldsymbol{\theta}_k - (\mathbf{J}_k^T\mathbf{J}_k)^{-1}\mathbf{J}_k^T\boldsymbol{f}_k \quad (8)$$

The method proposed by Jagersand [2] is of this kind. Piepmeier et al.'s method [3][4] also belongs to this kind, the difference is that it adds a time varying term to (8) so that it is fit for moving targets.

III. New Uncalibrated Visual Servoing Method

As stated in section I, there are many shortcomings of Gauss-Newton method for it drops the second order term directly. In this section, a new uncalibrated visual servoing method which doesn't drop the second order term directly but uses a secant to approximate it is presented. The approach to approximating the second order term is following that in the algorithm nl2sol [9], which is a very successful algorithm for solving nonlinear least squares problems.

A. *The approximation of the second order term*

It is to approximate $\mathbf{S}$, which is a symmetrical matrix. So, to approximate it better, the approximation also should be a symmetric. Besides, new information f_{k+1} and $\mathbf{J}_{k+1}$ should be incorporated into $\mathbf{S}_{k+1}$. A secant approximation is used here, that is letting the second-order approximant to transform the current change of $\boldsymbol{\theta}$ into the observed first-order change.

$$\begin{aligned}\mathbf{S}_{k+1}\Delta\boldsymbol{\theta}_k &= \sum f_i(\theta_{k+1})\nabla^2 f_i(\theta_{k+1})\Delta\boldsymbol{\theta}_k \\ &= \sum f_i(\theta_{k+1})(\nabla f_i(\theta_{k+1}) - \nabla f_i(\theta_k)) \\ &= J_{k+1}^T f_{k+1} - J_k^T f_{k+1}\end{aligned} \quad (9)$$

where $\Delta\boldsymbol{\theta}_k = \boldsymbol{\theta}_{k+1} - \boldsymbol{\theta}_k$. Let $\mathbf{z}_k = J_{k+1}^T f_{k+1} - J_k^T f_{k+1}$. Then, $\mathbf{S}_{k+1}$ should satisfy

$$\mathbf{S}_{k+1}\Delta\boldsymbol{\theta}_k = \mathbf{z}_k \quad (10)$$

There are many symmetrical matrix $\mathbf{S}_{k+1}$ satisfy (10). Here, we choose the one that is nearest to $\mathbf{S}_k$ because it destroys the least information stored in $\mathbf{S}_k$. Following the approach of nl2sol, obtain

$$\begin{aligned}\mathbf{S}_{k+1} = \mathbf{S}_k &+ \frac{(\mathbf{z}_k - \mathbf{S}_k\Delta\boldsymbol{\theta}_k)\mathbf{v}^T + \mathbf{v}(\mathbf{z}_k - \mathbf{S}_k\Delta\boldsymbol{\theta}_k)^T}{\Delta\boldsymbol{\theta}_k^T\mathbf{v}} \\ &- \frac{\Delta\boldsymbol{\theta}_k^T(\mathbf{z}_k - \mathbf{S}_k\Delta\boldsymbol{\theta}_k)\mathbf{v}\mathbf{v}^T}{(\Delta\boldsymbol{\theta}_k^T\mathbf{v})^2}\end{aligned} \quad (11)$$

where $\mathbf{v} = \Delta\mathbf{g}_k = J_{k+1}^T f_{k+1} - J_k^T f_k$.

B. *Trust region method*

The method using a quadratic model q to approximate the nonlinear function Φ is just locally convergent. In order to obtain global convergence, we use a trust region method [10].

$$\begin{aligned}\min &\frac{1}{2}\boldsymbol{f}_k{}^T\boldsymbol{f}_k + (\mathbf{J}_k^T\boldsymbol{f}_k)^T(\boldsymbol{\theta} - \boldsymbol{\theta}_k) \\ &+ \frac{1}{2}(\boldsymbol{\theta} - \boldsymbol{\theta}_k)^T(\mathbf{J}_k^T\mathbf{J}_k + \mathbf{S}_k)(\boldsymbol{\theta} - \boldsymbol{\theta}_k) \\ s.t.&\|\boldsymbol{\theta} - \boldsymbol{\theta}_k\| \le h_k\end{aligned} \quad (12)$$

By solving (12), obtain the control law

$$\theta_{k+1} = \theta_k - (J_k^T J_k + S_k + \alpha D^2)^{-1} J_k^T f_k \qquad (13)$$

where α is the Levenberg-Marquardt parameter and $\boldsymbol{D}$ is the diagonal scaling matrix. They are updated by More's approach [11].

If the quadratic model q_k can approximate the nonlinear function Φ very well, we increase the trust region, otherwise we decrease it. The trust region radius h_k is adjusted according to the ratio between the actual reduction of the function and the predicted reduction of it. The closer the ratio is to unity, the better q_k approximates Φ . The actual reduction of the function is

$$\Delta\Phi = \Phi_k - \Phi_{k+1} \qquad (14)$$

and the predicted reduction of the function is

$$\Delta q = \Phi_k - q_k \qquad (15)$$

Then, the ratio between the actual reduction and the predicted reduction is

$$r = \frac{\Delta\Phi}{\Delta q} \qquad (16)$$

The strategy to update the trust region radius is as follows

$$h_k = \begin{cases} 0.5\|\mathbf{D}\Delta\boldsymbol{\theta}\|_2, & r \le 0.25 \\ 2\|\mathbf{D}\Delta\boldsymbol{\theta}\|_2, & r \ge 0.75 \\ \|\mathbf{D}\Delta\boldsymbol{\theta}\|_2, & others \end{cases} \qquad (17)$$

C. The new uncalibrated visual servoing algorithm

The new uncalibrated visual servoing algorithm is as follows:

Step1. Set k=0. Given the initial image Jacobian $\hat{\boldsymbol{J}}_0$, the initial feature vector $\boldsymbol{y}_0$, the desired feature vector $\boldsymbol{y}^*$ and the initial second order term $\mathbf{S}_0 = 0$.

Step2. Compute the approximation of the Hessian by (3).

Step3. Compute the joint angles by (13).

Step4. Update the image Jacobian as (19) and (20) in section IV.

Step5. Calculate the ratio between actual reduction of the function and the predicted reduction by (14), (15), (16) and update the trust region radius by (17).

Step6. Update $\mathbf{S}$ by (11). k = k+1, return to step2.

The algorithm is based on trust region method [10], More's approach [11] and nl2sol method [9]. It is convergent and the analysis of the convergence can be seen in these works.

IV. Jacobian Estimation

In uncalibrated visual servoing, the Jacobian is unknown. Some researchers have proposed methods to approximate the image Jacobian by executing a set of calibration movements. However, the visual serving model is high degree of nonlinear. So, it is needed to make these calibration movements frequently. However, these movements are not necessary for our task, sometimes, even interfering with our task. Jagersand has proposed a Broyden's method for Jacobian estimation. However, when noise occurs in the system, the control method may be unstable in that it just uses the information in the latest step. Exponentially weighted recursive least squares (RLS) algorithm uses information of more steps. It is much more stable. Piepmeier et al. [3][4] have proposed a Jacobian estimation method using RLS algorithm. We use this method to estimate the coupled image Jacobian. The method is to construct a cost objective function

$$\Psi = \sum_{i=1}^{k} \lambda^{k-i} \left\| m_k(\theta_{i-1}) - m_{i-1}(\theta_{i-1}) \right\|^2 \qquad (18)$$

which is an exponentially weighted sum of the differences between the current quadratic model and past quadratic models, then, minimizing it. By doing this, we can get the approach to updating the Jacobian as follows:

$$\mathbf{J}_k = \mathbf{J}_{k-1} + \frac{((f_k - f_{k-1}) - \mathbf{J}_{k-1}\Delta\boldsymbol{\theta})\Delta\boldsymbol{\theta}^T \mathbf{P}_{k-1}}{\lambda + \Delta\boldsymbol{\theta}^T \mathbf{P}_{k-1}\Delta\boldsymbol{\theta}} \qquad (19)$$

$$\mathbf{P}_k = \frac{1}{\lambda}(\mathbf{P}_{k-1} - \frac{\mathbf{P}_{k-1}\Delta\boldsymbol{\theta}\Delta\boldsymbol{\theta}^T \mathbf{P}_{k-1}}{\lambda + \Delta\boldsymbol{\theta}^T \mathbf{P}_{k-1}\Delta\boldsymbol{\theta}}) \qquad (20)$$

where λ is the forgetting factor, $0 < \lambda \le 1$.

V. Method to Improve the Precision of Control

In uncalibrated visual servoing, many researchers are mainly concerned with the error in image plane. However, in some cases, the error of end-effector can be very large even if the error in image plane is zero or near zero, as it is shown in Fig. 1.

It is natural to think of arranging the cameras in parallel. However, cameras arranged in parallel or near in parallel are insensitive to the depth information. We propose a method to arrange the two cameras, arranging them vertically. For the convenience of analysis, assuming that the target is moving in the plane that the x coordinate is the same. As shown in Fig. 2, the target is moving the same distance L along the direction vertical and parallel to the optical axis from the initial position P_0 to P_1 and P_2, respectively. u_0, u_1 and u_2 are the corresponding positions in the image plane. From the geometry relation, we can get $u_0 = -\frac{f}{Z_0}Y_0$, $u_1 = -\frac{f}{Z_0}(Y_0 + L)$

and $u_2 = -\frac{f}{Z_0 - L} Y_0$, where f is the focus length. Then

$$|u_1 - u_0| = \frac{fL}{Z_0} \tag{21}$$

$$|u_2 - u_0| = \frac{fL}{Z_0} \bullet \frac{Y_0}{Z_0 - L} \tag{22}$$

When $Y_0 << Z_0 - L$, $|u_2 - u_0| << |u_1 - u_0|$. That is to say the camera is much sensitive to the movement vertical to the optical axis but less sensitive to the movement parallel to the optical axis in this situation. When two cameras arranged on parallel, both of them may be insensitive to the movement that parallel to the optical axis. However, when two cameras arranged vertically, the movement is parallel to the optical axis of one camera but vertical to the other. In this situation, one camera is insensitive the movement, but the other one is sensitive to it. The control precision in the workspace can be improved remarkably by this method when the target can be recognized on the two directions vertical to each other.

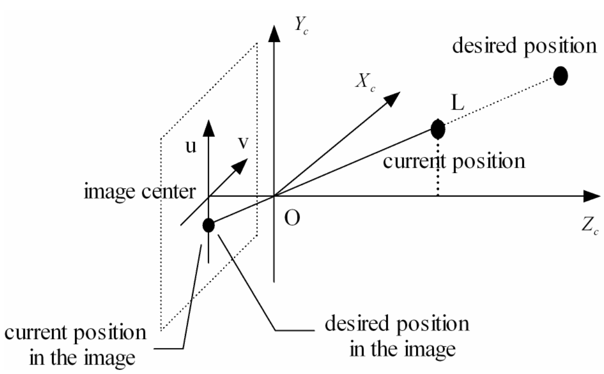

Figure 1. Camera model showing large error of end-effector while the error in image plane is zero or near zero

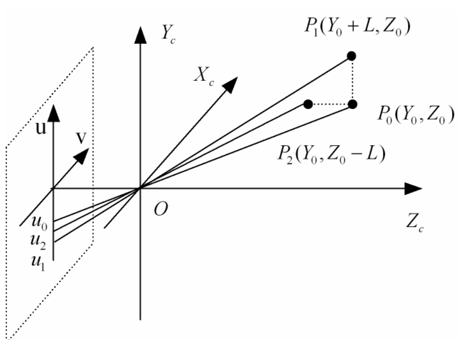

Figure 2. The changes of feature in the image plane when the target moving along the directions that are parallel and vertical to the optical axis, respectively

VI. SIMULATION RESULTS

Fig. 3 shows a three degree-of-freedom system that has been simulated to validate the new uncalibrated visual servoing controller and RLS algorithm as given in section III part C. The length of three links of the robot are L1=0.3 m, L2=0.4 m, L3=0.4 m. The vision of the robot is composed of two cameras. The focus length of the two camera are both 0.01 m. The image plane size is 640pixels$\times$480pixels. Zero-mean noise ± 1 pixel is added to the observed image. When the two cameras arranged nearly in parallel, translation and rotation of the two camera frames with respect to the robot base frame are set as follows:

$$ {}^b_1T = \begin{bmatrix} 1.0000 & 0.0000 & 0.0000 & 0.4453 \\ 0.0000 & 0.9988 & 0.0499 & 0.4307 \\ 0.0000 & -0.0499 & 0.9988 & -2.0000 \\ 0.0000 & 0.0000 & 0.0000 & 1.0000 \end{bmatrix} $$

$$ {}^b_2T = \begin{bmatrix} 1.0000 & 0.0000 & 0.0000 & 0.4453 \\ 0.0000 & 0.9988 & -0.0499 & 0.6307 \\ 0.0000 & 0.0499 & 0.9988 & -2.0000 \\ 0.0000 & 0.0000 & 0.0000 & 1.0000 \end{bmatrix} $$

When the two cameras arranged vertically, translation and rotation of the two camera frames with respect to the robot base frame are set as follows:

$$ {}^b_1T = \begin{bmatrix} 1.0000 & 0.0000 & 0.0000 & 0.4453 \\ 0.0000 & 1.0000 & 0.0000 & 0.5307 \\ 0.0000 & 0.0000 & 1.0000 & -2.0000 \\ 0.0000 & 0.0000 & 0.0000 & 1.0000 \end{bmatrix} $$

$$ {}^b_2T = \begin{bmatrix} 1.0000 & 0.0000 & 0.0000 & 0.4453 \\ 0.0000 & 0.0000 & -1.0000 & 2.5307 \\ 0.0000 & 1.0000 & 0.0000 & 0.0000 \\ 0.0000 & 0.0000 & 0.0000 & 1.0000 \end{bmatrix} $$

Given the initial image Jabobian

$$ \hat{\mathbf{J}}(0) = \begin{bmatrix} -13.0000 & 150.4202 & -80.7172 \\ -180.3290 & -40.3744 & 5.3524 \\ 3.0000 & 143.5632 & -70.3389 \\ -123.1090 & -130.1153 & 30.1837 \end{bmatrix} $$

By taking the new uncalibrated visual servoing method stated in section III, it is not needed to know the Jacobian exactly but just given a roughly estimated Jacobian. The real initial Jacobian is

$$\mathbf{J}(0) = \begin{bmatrix} 0.0000 & 173.4202 & -128.7172 \\ -154.3290 & -66.3744 & 10.3524 \\ 0.0000 & 171.5632 & -127.3389 \\ -144.1090 & -78.1153 & 12.1837 \end{bmatrix}$$

Though $\hat{\mathbf{J}}(0)$ is much different from $\mathbf{J}(0)$, the simulation results bellow demonstrate that the precision of robot control is still very high.

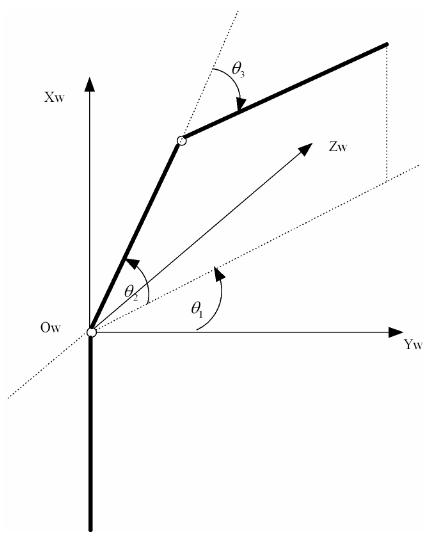

Figure 3. Three-degree-of-freedom robot and the world coordinate

We test the Gauss-Newton uncalibrated visual servoing method and the new uncalibrated visual servoing method in small and large residual case, respectively. The initial position of the end-effector is $[0.4453\ 0.2654\ 0.4596]^T$ m, the corresponding joint angles is $[60\ 70\ 60]^T$ degree. In the small residual case, the desired position of the end-effector is $[0.3266\ 0.4502\ 0.5365]^T$, the corresponding joint angles is $[50\ 40\ 30]^T$ degree. In the large residual case, the desired position of the end-effector is $[0.6741\ 0.4035\ 0.1469]^T$, the corresponding joint angles is $[20\ 60\ 5]^T$ degree. Jacobian estimation all uses RLS method. Fig. 4 and Fig. 5 show the results of Gauss-Newton and new uncalibrated visual servoing method in small residual case. Fig. 6 and Fig. 7 show the results of the two methods in large residual case. Comparing Fig. 4, Fig. 5, Fig. 6 and Fig. 7, it can be found that in small residual cases the performance of Gauss-Newton uncalibrated visual servoing is good, but in large residual cases Gauss-Newton uncalibrated visual servoing can't converge to the desired value, the performance of new uncalibrated visual servoing method is quite good in large residual cases, even in small residual cases the performance new uncalibrate visual servoing method is superior to Gauss-Newton uncalibrated visual servoing method.

Though as show in Fig. 5 and Fig. 7 the error in image plane is very small, if the two cameras are arranged in parallel the error of end-effector in the workspace can be very large(see table I). Comparing table I and table II, it can be found that by taking the method to improve the control precision stated in section V the precision can be improved greatly.

TABLE I. END-EFFECTOR ERRORS WITH CAMERAS IN PARALLEL [10^{-4}m]

Errors	**1**	**2**	**3**	**4**	**5**	**6**	**Standard Deviation**
x error	-15	-13	-20	-33	-46	-23	30.09
y error	8.85	9.3	7.21	17	29	13	17.41
z error	-153	-119	-162	-279	-233	-235	224.13

TABLE II. END-EFFECTOR ERRORS WITH CAMERAS IN VERTICAL [10^{-4}m]

Errors	**1**	**2**	**3**	**4**	**5**	**6**	**Standard Deviation**
x error	-7.49	-7.80	-15	-6.98	-2.38	-8.51	9.68
y error	-18	-14	12	-13	-14	-5.58	14.56
z error	11	-5.13	-3.53	-15	2.52	-3.92	9.02

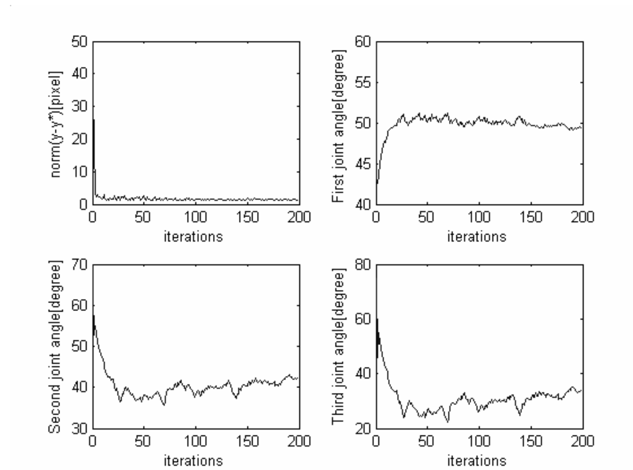

Figure 4. Simulation result of Gauss-Newton uncalibrated visual servoing method in small residual case

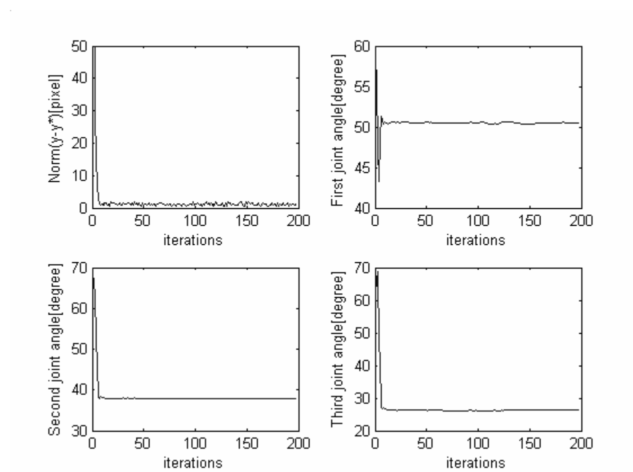

Figure 5. Simulation result of new uncalibrated visual servoing method in small residual case

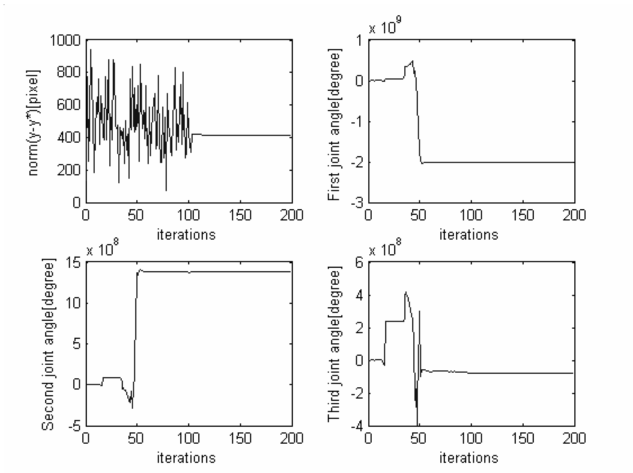

Figure 6. Simulation result of Gauss-Newton uncalibrated visual servoing method in large residual case

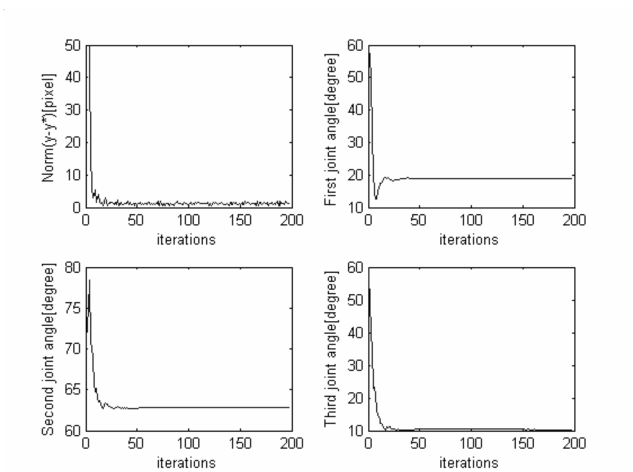

Figure 7. Simulation result of new uncalibrated visual servoing method in large residual case

VII. Conclusions

In this paper, A RLS algorithm is used to estimate the coupled image Jacobian. So, it is not needed to calibrate the camera and the robot. This is very useful in the cases where it is hard or unable to calibrate the camera and the robot.

A new uncalibrated visual servoing method for large residual problems is presented in this paper. It uses a secant to approximate the second order term rather than dropping it directly. That is to say, it is a more accurate model of the nonlinear function. So, the convergence is much faster and much more stable than the Guass-Newton uncalibrated visual servoing method, especially in large residual cases.

A trust region method is used. It guarantees that the algorithm is globally convergent and the convergence is as fast as possible.

For static object with two cameras, a method to improve the control precision in the workspace by arranging the two cameras vertically is proposed. This paper discusses uncalibrated visual servoing. It just needs to make the two cameras roughly vertical. Even though, it can improve the precision in the workspace than arranging them in parallel or near parallel. This is the guideline for the arranging of the cameras.

A three degree-of-freedom system has been simulated to validate the algorithm. The simulation results demonstrate that the algorithm is quite fast and stable and that the control precision is very high.

References

[1] K. Hosoda and M. Asada, "Versatile Visual servoing without knowledge of true jacobian", Proceedings of the IEEE/RSJ International Conference on Intelligent Robots and Systems, Munich, Germany, Sept. 1994, pp. 186–193.

[2] M. Jagersand, "Visual servoing using trust region methods and estimation of the full coupled visual-motor jacobian", In Proc. of IASTED Applications of Control and Robotics, 1996.

[3] J.A. Piepmeier, G.V. Mcmurray and H. Lipkin, "A dynamic quasi-newton method for uncalibrated visual servoing", Proceedings of the 1999 IEEE International Conference on Robotics and Automation (WOMPAT), Detroit, May 1999, pp. 1595–1600.

[4] J.A. Piepmeier, G.V. Mcmurray and H. Lipkin, "uncalibrated dynamic visual servoing", IEEE transactions on robotics and automation, vol. 20, no. 1, pp.143–147, Feb. 2004.

[5] P. Jiang, L.C.A. Bamforth, Z.R. Feng, J.E.F. Baruch and Y.Q. Chen, "Indirect Iterative Learning Control for a Discrete Visual Servo Without a Camera-Robot Model", IEEE transactions on systems, man, and cybernetics- part b: cybernetics, vol. 37, no. 4, pp.863–876, Aug. 2007.

[6] Y.H. Liu, H.S. Wang, C.Y. Wang and K.K. Lam, "Uncalibrated Visual servoing of robots using a depth-independent interaction matrix", IEEE transactions on robotics, vol. 22, no. 4, pp. 804-817, Aug. 2006.

[7] K. Miura, K. Hashimoto, J. Gangloff and M. de Mathelin, "Visual servoing without jacobian using modified simplex optimization", Proceedings of the 2005 IEEE International Conference on Robotics and Automation, Apr. 2005, pp. 3504–3509.

[8] G.W. Kim, B.H. Lee and M.S. Kim, "Uncalibrated Visual Servoing Technique Using Large Residual", Proceedings of the 2003 IEEE International Conference on Robotics and Automation, Sept. 2003, vol. 3, pp. 3315–3320.

[9] J.E. Dennis, D.M. Gay and R.E. Walsh, "An Adaptive Nonlinear Least-Squares Algorithm", ACM Transactions on Mathematical Software (TOMS), vol. 7, no. 3, pp. 348-368, Sept. 1981.

[10] R. Fletcher, Practical Methods of Optimization, Second Edition, John Wiley & Sons, 1987.

[11] J.J. More, "The Levenberg-Marquardt algorithm: Implementation and theory", Lecture Notes in Mathematics, Berlin: Springer, vol. 630, pp. 105-116, 1978.